

THE SHAPE EFFECT ON THE MELTING PROCESS OF ALUMINUM NANOWIRES: A MOLECULAR DYNAMICS STUDY

Unal Domekeli^{1,*}, Murat Celtek²

¹Dept. of Physics, Trakya University, 22030, Edirne – Türkiye ²Faculty of Education, Trakya University, 22030, Edirne – Türkiye *Corresponding author: unaldomekeli@trakya.edu.tr

Abstract

Nanowires, one of the nanostructured materials, are extensively used due to their unique performance and impact on the next generation industry. Nanowires have received significant attention from the nanotechnology research and application community. Therefore, it is considered a promising candidate for future nano-scale devices that are expected to shrink significantly in size. In this study, we investigated the effects of cross-sectional shape on the melting behavior of Aluminum (Al) nanowires using molecular dynamics (MD) simulation technique with embedded atom potentials (EAM). In the simulations, cylindrical and square cross-section nanowire models were used to observe the cross-section effect. During the heating process, some thermal, structural and dynamic properties of the system were calculated. The results show that the cross-sectional shape has an effect on the melting behavior of Al nanowires, but this effect does not create significant differences. Moreover, above melting temperatures, a thickening occurs in the region corresponding to the nanowire's midsection. After a critical temperature value, the nanowire transforms into nanoparticle form.

Keywords: Al nanowire, EAM, MD simulations, shape effect, melting behavior.

INTRODUCTION

There has recently been a great deal of interest in metallic nanowires (MNWs) from a technological perspective [1–3]. Due to their high surface-to-volume ratio, MNWs exhibit unique physical and chemical properties that distinguish them from their bulk counterparts [4]. MNWs produced using different growth methods have a wide range of applications, particularly in electronics, optoelectronics and biosensors [5]. However, heat generation is an inevitable by-product of electronic devices operating. The thermal behavior of MNWs significantly impacts the performance and reliability of nano-electronic devices and other applications. Therefore, it is crucial to understand the thermal stability structural properties of MNWs at different temperatures [1]. Atomic simulation techniques are a powerful tool for investigating the thermal stability and structural properties of MNWs. There are numerous molecular dynamics simulation studies available on the melting behavior of MNWs [6–13]. For example, Yang et al. [8] investigated the shape effect on the melting behavior of vanadium NWs using MD simulation. They reported that the shape of the wire had a strong influence on NW melting. Ridings et al. [11] studied the surface melting of nickel (Ni) and Al NWs MD simulation and the Landau model. They indicated that surface anisotropy plays a key role in the melting of metal NWs and their surfaces. In this study, we investigated in detail the melting mechanism of Al NWs with different cross-sectional shapes during the heating process using MD simulations with EAM force field.

EXPOSITION

EAM potentials are frequently used in MD simulations, as they can accurately describe interatomic interactions in metals and alloys. According to the EAM model, the total energy of a system consisting of *N* atoms can be expressed as follows [14,15]:

$$E_{T} = \sum_{i=1}^{N} \left[\frac{1}{2} \sum_{i \neq j}^{N} \phi(r_{ij}) + F_{i}(\rho_{i}) \right]$$
 (1)

where $\phi(r_{ij})$ is the pair interaction potential energy function and $F_i(\rho_i)$ is the energy required to place an atom i at a lattice point where the electronic charge density ρ_i is located. This energy is known as the embedding energy. The ρ_i expression is the sum of the atomic charge densities of the neighboring atoms surrounding atom $i. r_{ij}$ is the distance between atoms i and j. In this study, the EAM potential dataset developed by Sheng [16] was used to identify Al-Al interactions. The parallel code DLPOLY [17] MD simulation package was used to investigate the melting process of Al NWs. To investigate the shape effect on the melting behavior of Al NWs, we studied NWs with cylindrical and square crosssections. These model NWs, shown in Figure 1, were obtained from the ideal facecentered cubic (fcc) crystal structure using square and cylindrical cross-section cutting methods. To eliminate the size effect, we took the diameter (d) of the cylindrical NW (CNW) and the square section length (d) of the square NW (SNW) as the same. Furthermore, the heights (H) of both NWs were taken as equal. The size and number of atoms information of the model NWs are listed in Table 1.

Table 1. The d and H lengths and N number of atoms of Al NWs.

Symbol	N	d(nm)	H(nm)
CNW	12040	4.0	16.2
SNW	16000	4.0	16.2

To account for the effects of the surface on the Al NWs, periodic boundary conditions were applied only along the [001] z-axis in the MD simulations. Initial samples containing atoms in ideal fcc positions were relaxed using the following annealing cycle: the system was first heated to 300 K at a rate of 0.05 K/ps and then cooled to 0 K at a rate of 0.05 K/ps. The NWs were simulated using the NVT ensemble under constant volume and temperature conditions. The NWs were subjected to a heating process consisting of a series of MD simulations, with the temperature increased by $\Delta T = 100 \text{ K}$ from 100 K to 1200 K. In the vicinity of the melting point, the temperature increases were reduced to $\Delta T = 10 \text{ K}$ to account for large temperature fluctuations. For each simulation, equilibration was performed for 100 ps, followed by a production time of 50 ps, to produce time-based properties at each temperature. The Newtonian equations of motion were integrated using the Leapfrog Verlet method with a time step of 1 fs. The temperature and pressure of the system were controlled by the Nose-Hoover thermostat [18] and the Berendsen barostat [19], respectively.

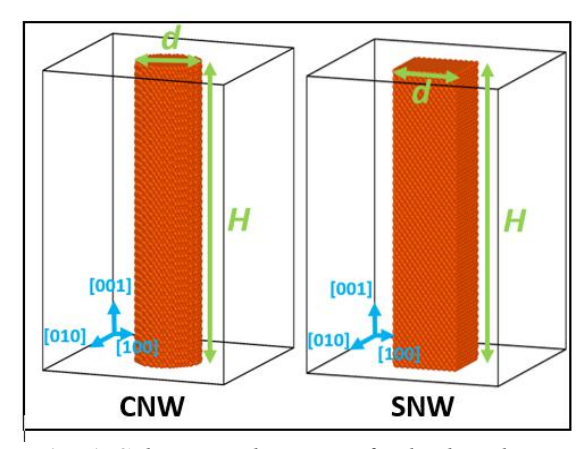


Fig. 1. Schematic diagram of cylindrical NW (CNW) and square NW (SNW).

The simplest way to determine the melting temperature at which a first-order phase transition occurs in a system is to monitor how the total energy changes with temperature. Figure 2 shows the temperature-dependent variation in total energy for Al NWs. At low temperatures, the total energy of both NWs increases linearly with temperature. At higher temperatures,

however, a sudden jump is observed in both energy curves. This jump is defined as the melting temperature (T_m), which is the temperature at which the system undergoes phase transition. first-order temperatures at which a sudden jump in the energy curve is observed are 750 K and 760 K for CNW and SNW, respectively. The total energies of liquid CNW and SNW both increase linearly with temperature, but then drop abruptly at 790 K and 830 K, respectively. At temperatures higher than these, the energy curves continue to increase linearly with temperature. Also, the energy of CNW is greater than that of SNW, which suggests that SNW is more thermally stable.

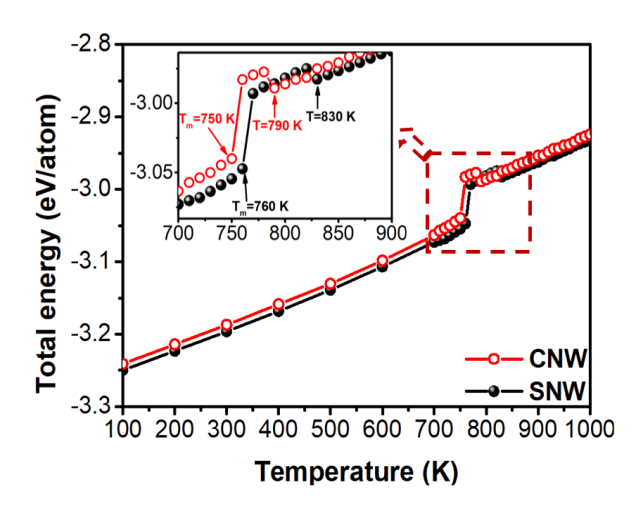


Fig. 2. Temperature-dependence of total energy for Al NWs.

Table 2 shows a comparison of the T_m and heat of fusion (ΔH_m) values obtained from MD simulations for Al CNW and SNW with those for the bulk. The melting temperature was calculated from the energy difference between the solid and liquid phases in the total energy curve. Details of this calculation and the results for the bulk can be found in our previous work [15]. The T_m and ΔH_m values of both NWs are lower than those of the bulk. The T_m and ΔH_m values of SNW are higher than those of CNW.

Table 2. T_m and ΔH_m obtained from MD simulation for Al NWs and bulk system.

Symbol	$T_m(K)$	$\Delta H_{\rm m} (Kj/{ m mol})$
CNW	750	6.70
SNW	760	7.44
Bulk	930	8.81

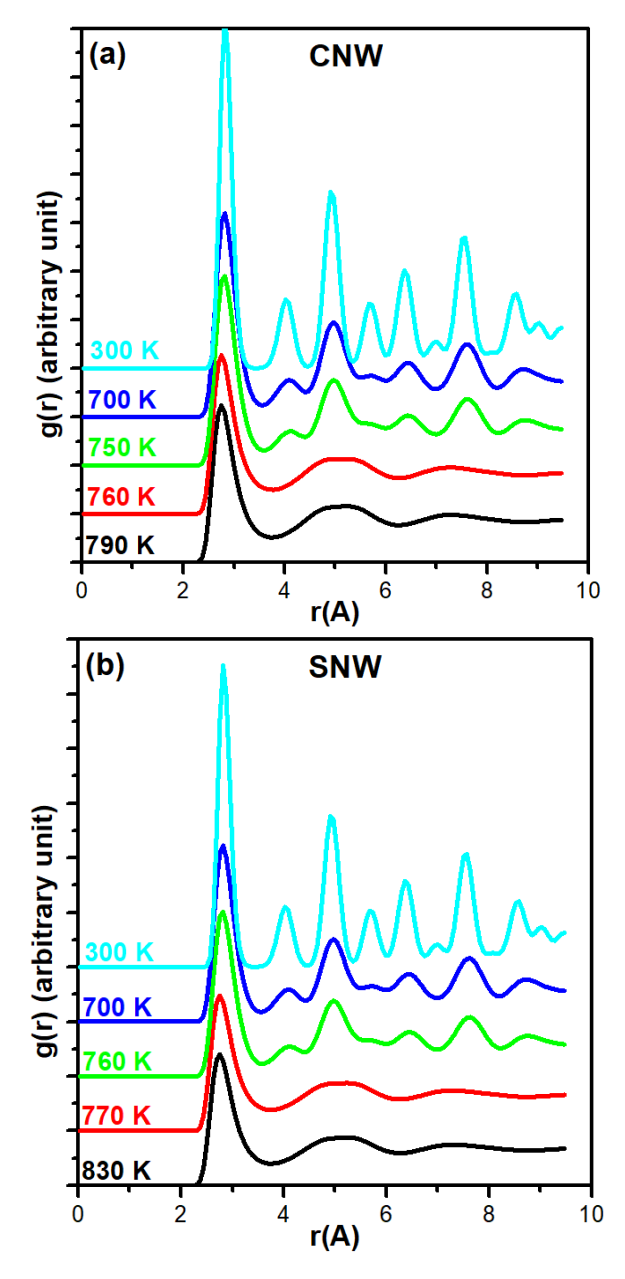


Fig. 3. PDFs of Al (a) CNW (b) SNW at different temperatures during the heating process.

We studied the structural evolution of Al NWs during the heating process using the pair distribution function (PDF). The PDF, g(r), is defined as [20]:

$$g(r) = \frac{\Omega}{N^2} \langle \left(\sum_{i=1}^{N_i} n_i \right) / 4\pi r^2 \Delta r \rangle$$
 (2)

where is Ω the volume of unit cell, and N is the number of atoms in simulation box. Figure 3 shows the PDFs of the Al CNW and SNW at different temperatures. At 300 K, both NW PDFs exhibit behavior that is characteristic of an FCC crystal structure. As increases, the temperature the **PDF** amplitudes decrease while the peak widths increase. At 760 K for the CNW and 770 K for the SNW, the PDFs exhibit behavior indicative of a liquid phase. At temperatures where a sudden drop in the energy curve is observed, the PDFs of both NWs continue to exhibit liquid phase behavior.

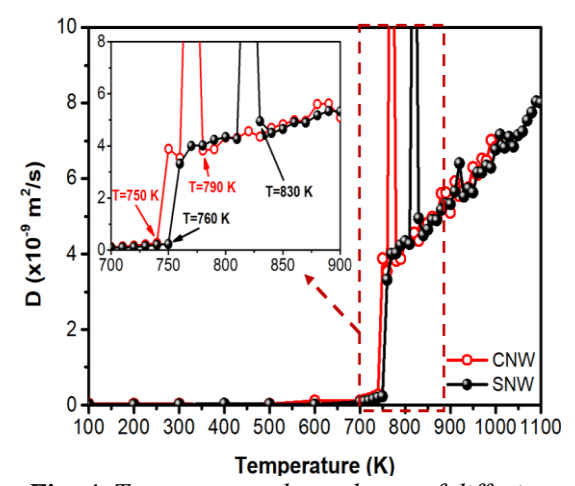


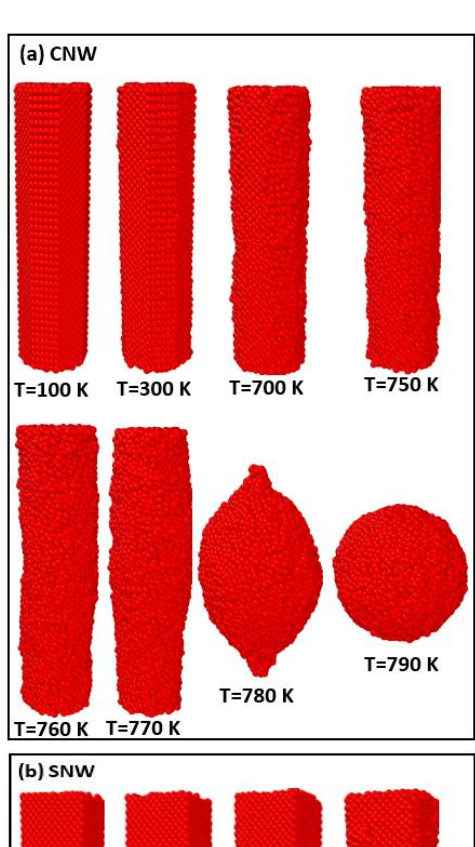
Fig. 4. Temperature-dependence of diffusion coefficients for Al CNW and SNW.

A first order phase transition can be identified by examining how diffusivity a measure of the mobility of the atoms in the system varies with temperature. coefficient diffusion encompasses system's dynamic properties and can be derived from the positions and velocities of atomic projections in MD simulations. It is expected that the diffusion coefficient will be related to the path of a particle over time, indicating that the square mean displacement (MSD) will be linearly related at large time values. The diffusion coefficient, D, can be calculated using the Einstein correlation [21]:

$$D = \lim_{t \to \infty} \frac{MSD}{6t} \tag{3}$$

where t is the diffusion time, MSD of the atom in the MD simulations can be described as [21]:

$$MSD = \frac{1}{N} \sum_{i=1}^{N} |r_i(t + t_o) - r_i(t_o)|^2$$
 (4)



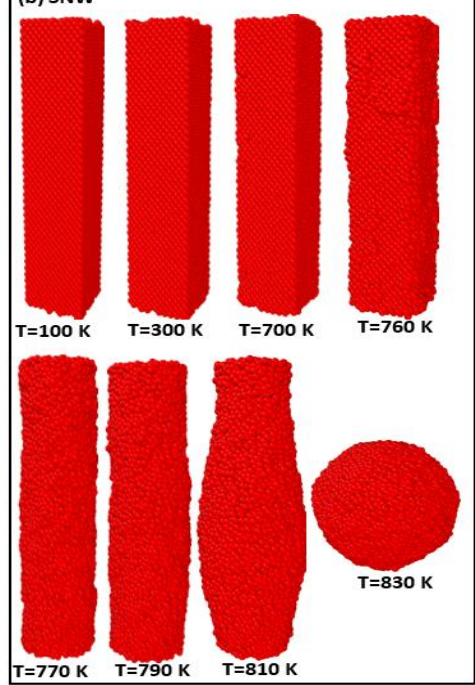


Fig. 5. Snapshots of Al (a) CNW and (b) SNW at different temperatures during heating.

where $r_i(t_o)$ is the position vector of the *i*th atom for the system in its initial configuration and $r_i(t)$ is the position vector of ith atom at time t. Figure 4 illustrates the temperature-dependent variation in the diffusion coefficients of Al CNW and SNW. The diffusion coefficients of both NWs are almost zero from 100 K to 700 K. While an increase in the diffusion coefficients was observed starting from 700 K, a sudden increase in the diffusion coefficient was observed at the melting temperatures of both NWs. This behavior suggests that the atoms in the system have detached from their lattice points and are moving freely, as they would in a liquid. Additionally, there is a sudden change in diffusion coefficients at 790 K for CNW and at 830 K for SNW.

Figure 5 shows snapshots of atomic coordinates obtained from MD simulations at different temperatures for Al CNW and SNW. From 100 K to 300 K, both NWs maintain their fcc crystal structure. At 700 K, the atoms on the surface of the CNW begin to leave the lattice points in the crystalline arrangement, but the surface atoms of the SNW still maintain their crystalline structure. At melting temperatures, the atoms on the surface of both NWs move randomly, as in the liquid phase. Above their melting temperatures, a thickening occurs in the middle section of the wire for both NWs. CNW and SNW transform into spherical nanoparticles at 790 and 830 K, respectively. This explains the sudden drop in the energy curve and diffusion coefficients. Since the geometric structure of a spherical nanoparticle (NP) is more stable than that of a NW, the observed decrease in the energy curve is an expected result.

CONCLUSION

In this study, the effect of cross-sectional shape on the melting behavior of Al NWs was investigated in detail using MD simulations with EAM potentials. The results indicated that the T_m and ΔH_m values of both NWs are lower than those of their bulk. The T_m and ΔH_m values of SNW are

higher than those of CNW. Furthermore, the total energy of SNW is lower than that of CNW. This indicates that SNW is thermally more stable than CNW. Above the melting point, thickening occurs in the middle region of the wire for both NWs. The cause triggering this thickening may be surface melting occurring in the NW. For both CNW and SNW, at critical temperatures (Tc), the NW transforms into the NP form. The Tc values for CNW and SNW are 790 K and 830 K, respectively. Consequently, it can be stated that the cross-sectional shape factor affects the melting behavior of Al NWs.

Funding No funding support has been received from any institution or person.

Acknowledgments: We would like to thank Trakya University Rectorate for giving permission and contributing to present this study as a paper.

REFERENCE

- [1] J. Zhang, X. Wang, Y. Zhu, T. Shi, Z. Tang, M. Li, G. Liao, Molecular dynamics simulation of the melting behavior of copper nanorod, Comput. Mater. Sci. 143 (2018) 248–254.
- [2] L. Cademartiri, G.A. Ozin, Ultrathin Nanowires—A Materials Chemistry Perspective, Adv. Mater. 21 (2009) 1013– 1020.
- [3] M. Law, J. Goldberger, P. Yang, Semiconductor Nanowires and Nanotubes, Annu. Rev. Mater. Res. 34 (2004) 83–122.
- [4] B. Issa, I. Obaidat, B. Albiss, Y. Haik, Magnetic Nanoparticles: Surface Effects and Properties Related to Biomedicine Applications, Int. J. Mol. Sci. 14 (2013) 21266–21305.
- [5] D.S. Hecht, L. Hu, G. Irvin, Emerging Transparent Electrodes Based on Thin Films of Carbon Nanotubes, Graphene, and Metallic Nanostructures, Adv. Mater. 23 (2011) 1482–1513.
- [6] O. Gülseren, F. Ercolessi, E. Tosatti, Noncrystalline Structures of Ultrathin Unsupported Nanowires, Phys. Rev. Lett. 80 (1998) 3775–3778.
- [7] S.S. Dalgic, U. Domekeli, Molecular dynamics simulation studies on melting of

- Sn nanowires, J. Optoelectron. Adv. Mater. 13 (2011) 1570–1576.
- [8] X.Y. Yang, X.J. Chen, Atomistic simulation on the shape dependence of the melting behavior of V nanowire, Eur. Phys. J. D 66 (2012) 128.
- [9] Zhou Guo-Rong, Teng Xin-Ying, Wang Yan, Geng Hao-Ran, Hur Bo-Young, Size effect on the freezing behavior of aluminum nanowires, Acta Phys. Sin. 61 (2012) 066101.
- [10] W.X. Zhang, C. He, Melting of Cu Nanowires: A Study Using Molecular Dynamics Simulation, J. Phys. Chem. C 114 (2010) 8717–8720.
- [11] K.M. Ridings, T.S. Aldershof, S.C. Hendy, Surface melting and breakup of metal nanowires: Theory and molecular dynamics simulation, J. Chem. Phys. 150 (2019).
- [12] K.M. Ridings, S.C. Hendy, Nanowire melting modes during the solid–liquid phase transition: theory and molecular dynamics simulations, Sci. Rep. 12 (2022) 20052.
- [13] M. Javanbakht, S.S. Eskandari, M. Silani, Surface induced melting of long Al nanowires: phase field model and simulations for pressure loading and without it, Nanotechnology 33 (2022) 425705.
- [14] M.S. Daw, M.I. Baskes, Embedded-atom method: Derivation and application to impurities, surfaces, and other defects in

- metals, Phys. Rev. B 29 (1984) 6443–6453.
- [15] U. Domekeli, M. Celtek, Structural and dynamic properties of aluminum nanoparticles during the melting process, UNITECH 2024 Sel. Pap. (2024).
- [16] H. Sheng, EAM potentials, (2024). https://sites.google.com/site/eampotentials/table/al.
- [17] W. Smith, T.R. Forester, DLPOLY 2.0: A general-purpose parallel molecular dynamics simulation package, J. Mol. Graph. 14 (1996) 136–141.
- [18] S. Nose, A unified formulation of the constant temperature molecular dynamics methods, J. Chem. Phys. 81 (1984) 511–519.
- [19] H.J.C. Berendsen, J.P.M. Postma, W.F. van Gunsteren, A. DiNola, J.R. Haak, Molecular dynamics with coupling to an external bath, J. Chem. Phys. 81 (1984) 3684–3690.
- [20] Sedat Sengul, Unal Domekeli, Murat Celtek, Melting Behavior of Pb Nanowires: Molecular Dynamics Dimulations, International Scientific Conference UNITECH 2020, Gabrovo, (2020), p. II-381.
- [21] U. Domekeli, M. Celtek, Melting Mechanism of Cylindrical Molybdenum Nanowire: A Molecular Dynamics Simulation Study, UNITECH 2024—Sel. Pap. (2024).